**Biogeosciences
Discussions**

The stoichiometric ratio during biological removal of inorganic carbon and nutrient in the Mississippi River plume and adjacent continental shelf

W.-J. Huang[1], W.-J. Cai[1], R. T. Powell[2], S. E. Lohrenz[3], Y. Wang[1], L.-Q. Jiang[1,*], and C. S. Hopkinson[1]

[1]Department of Marine Sciences, University of Georgia, Athens, Georgia, 30602, USA
[2]Central Carolina Community College, Sanford, North Carolina, 27330, USA
[3]Department of Fisheries Oceanography, University of Massachusetts Dartmouth, New Bedford, MA 02744, USA
[*]now at: Earth Resources Technology 6100 Frost Place, Suite A Laurel, MD 20707, USA

Correspondence to: W.-J. Cai (wcai@uga.edu)

Title Page

Abstract | Introduction

Conclusions | References

Tables | Figures

|◀ | ▶|

◀ | ▶

Back | Close

Full Screen / Esc

Printer-friendly Version

Interactive Discussion

Abstract

The stoichiometric ratios of dissolved inorganic carbon (DIC) and nutrients during biological removal have been widely assumed to follow the Redfield ratios (especially the C/N ratio) in large river plume ecosystems. However, this assumption has not been systematically examined and documented because DIC and nutrients are rarely studied simultaneously in a river plume area, a region in which they can be affected by strong river-ocean mixing as well as intense biological activity. We examined stoichiometric ratios of DIC, total alkalinity (TA), and nutrients (NO_3, PO_4^{3-} and $Si(OH)_4$) data during biological removal in the Mississippi River plume and adjacent continental shelf in June 2003 and August 2004 with biological removals defined as the difference between measured values and values predicted on the basis of conservative mixing determined using a multi-endmember mixing model. Despite complex physical and biogeochemical influences, relationships between DIC and nutrients were strongly dependent on salinity range and geographic location, and influenced by biological removal. Lower C/Si and N/Si ratios in one nearshore area were attributed to a potential silicate source induced by water exchange with coastal salt marshes. When net biological uptake was separated from river-ocean mixing and the impact of marshes and bays excluded, stoichiometric ratios of C/N/Si were similar to the Redfield ratios, thus supporting the applicability of the Redfield-type C/N/Si ratios as a principle in river-plume biogeochemical models.

1 Introduction

Large river plumes and surrounding waters are important as processors of terrestrially-derived biogenic elements, such as carbon, nitrogen, phosphorus and silicon as these materials are transported from land to the ocean. Redfield (1958) first proposed a biological control for a fixed C/N/P stoichiometry of marine plankton, and subsequently inorganic and organic stoichiometry has been examined in freshwater (Hecky et al.,

1993), marginal seas (Frigstad et al., 2011; Hupe and Karstensen, 2000), and the open ocean (Hopkinson and Vallino, 2005; Li et al., 2000; Li and Peng, 2002). These studies have led to an improved understanding of the relationships between nutrient availability and biogeochemical processes such as photosynthesis and remineralization in all aquatic systems. Redfield stoichiometric ratios have been applied in coastal ocean biogeochemical models in the Northern Gulf of Mexico (Fennel et al., 2011; Green et al., 2006, 2008), and used in linking river nutrient loading with sea surface partial pressure of carbon dioxide (Gypens et al., 2004) and ocean acidification (Borges and Gypens, 2010). These studies have widely assumed that dissolved inorganic carbon (DIC) uptake and nitrogen removal ratio in the water column follows the Redfield value (i.e., 106/16 by atoms). However, to our knowledge, a detailed analysis of field data and thus a field validation of the stoichiometric relationship between DIC uptake and inorganic nitrogen, phosphate and silicate removals are lacking for large river plumes, especially when variability of C/N/P stoichiometry of microalgae and of assimilation have been observed (Geider and La Roche, 2002; Donald et al., 2001). This is largely due to the fact that nutrient and DIC removal are rarely reported simultaneously for river plumes, although such information is critical to efforts to characterize factors controlling carbon sinks and sources in these regions.

Intense biological processes have been reported in large river plumes and can include high rates of uptake of nutrients (DeMaster and Pope, 1996; Lohrenz et al., 1997) and carbon (Ternon et al., 2000; Cai, 2003). However, DIC and nutrient concentrations in plumes are also affected by temporally variable and spatially heterogeneous river-ocean mixing dynamics, which can complicate the interpretation of the biological signals (as opposed to those within spatially bounded estuaries, Gazeau et al., 2005). In addition, there are extensive marshes located along the Louisiana coast, which could be significant sources of dissolved nutrients such as Si (Struyf et al., 2006) but are usually neglected when considered in relationship to the Mississippi River loading. This potential Si source could further complicate the relationship between DIC and nutrients in adjacent shelf and river plume waters. Therefore, knowledge of water mixing

and elemental exchange between linked river-estuary-plume-shelf systems is critical to fully understanding plume biological dynamics, their relationship to the stoichiometry of C/N/P/Si uptake, and ultimately the forecasting and management of these systems in a global context.

To examine the stoichiometric ratios of C/N/P/Si uptake in the Mississippi River plume, we first considered the conservative mixing properties of multiple water masses by using a multi-endmember model. Using this approach, we then calculated the biological removals of DIC and inorganic nitrogen, phosphate, and silicate. Additionally, we examined DIC, nutrients, and their biological removals in relationship to geographic sampling locations to discern potential effects of the adjacent coastal marshes on uptake stoichiometry.

2 Methods

2.1 Site description

The Mississippi River splits into the Mississippi and the Atchafalaya rivers before emptying onto the Louisiana shelf. The Atchafalaya River receives about 30 % of the Mississippi River water (van Heerden et al., 1983) with some additional inputs from a local river, the Red River. These rivers account for the majority of freshwater inputs to the Louisiana shelf. Average discharge of the Mississippi River was $17\,300\,\mathrm{m^3\,s^{-1}}$ during 24–29 June 2003 and $9000\,\mathrm{m^3\,s^{-1}}$ during 9–12 August 2004. During both periods, river discharge was declining (Fig. 1). The Barataria estuary is located to the west of the Mississippi River and just to the north of the river plume in the Louisiana Bight (Fig. 2a). The Barataria Bay is a large, shallow fresh-salt water dominated wetland estuary with rainwater as its only source of fresh-water except for occasional inputs from the Davis Pond river diversion near its southeast edge ($\sim 250\,\mathrm{m^3\,s^{-1}}$ when operative). Li et al. (2011) reported a net outflow to the Louisiana Bight of $380\,\mathrm{m^3\,s^{-1}}$ over a 24 h period. However, strong tidal exchange also introduces Mississippi River-influenced shelf water into the estuary.

The dominant coastal current on the Louisiana shelf generally flows to the west but a clockwise eddy occurs adjacent to the Birdfoot (Balize) Delta in the Louisiana Bight that advect Mississippi River dominated shelf water to the vicinity of inlets connected to the Barataria Bay (Morey et al., 2003; Walker et al., 2005; Das et al., 2010). Thus, some Mississippi River water emptying from Southwest Pass may, during the process of mixing with shelf water masses, enter the Barataria Bay (Li et al., 2011).

2.2 Sampling

Two cruises were conducted on board the R/V *Pelican* in June 2003 and August 2004 in the Louisiana Bight and adjacent shelf. The first cruise focused on the Louisiana Bight region while the second cruise covered a broader area extending towards Texas and including the Atchafalaya plume region. The first cruise followed a lower Mississippi River cruise during 20–24 June 2003 (Dagg et al., 2005). TA and DIC concentrations were determined for water samples collected either from Niskin bottles mounted on a carousel included as part of the vertical profiling package or from the ship's flow-through system from about 1 m depth via a floating water intake. Nutrients, including NO_3, PO_4^{3-}, and $Si(OH)_4$ were determined for samples collected from Niskin bottles or from the flow-through system on the first cruise and only from Niskin bottles on the second cruise. Nutrient analyses were performed as described by Dagg et al. (2008).

DIC and TA samples were collected using 120 ml glass bottles thoroughly flushed with sample with extensive overflow (> 60 ml). DIC was measured shortly after the cruise by acidifying 0.5 ml of sample and quantifying the released carbon dioxide using an infrared detector (LI-COR® 6252). This method had a precision of 0.1 % (Cai and Wang, 1998). TA was determined by the Gran titration on 16 ml of sample using an automated system equipped with Kloehn digital syringe pumps with a precision of 0.1 % (Cai et al., 2010; Cai and Wang, 1998).

2.3 Estimation of stoichiometry

To examine the stoichiometry of net carbon and nutrient uptake, we applied a three-endmember mixing model to the data of August 2004, which covered a larger area, and a two-endmember mixing model to June 2003 data which covered a smaller area in the vicinity of the Mississippi River outflow in the Louisiana Bight. Similar approaches have been applied using both a two-endmember or an endmember-free model to estimate the Redfield ratio or stoichiometry of remineralization in open ocean waters (Takahashi et al., 1985; Anderson and Sarmiento, 1994; Li and Peng, 2002; Li et al., 2000). A multi-endmember model was used to estimate the Redfield stoichiometry in the Arabian Sea (Hupe and Karstensen, 2000) to accommodate the fact that mixing gradients are stronger in coastal waters influenced by freshwater inputs than in open ocean waters. Further justification for the use of the different endmember models in the present study is given in Sect. 3.1. In the following paragraphs, we lay down a framework for our approach.

In a three-endmember mixing model, the sum of the fractions from all the contributing endmembers is unity (Eq. 1). Since salinity is a conservative tracer in this model, the salinity for a given water parcel can be estimated as the sum of fractional contributions from the various endmembers (Eq. 2).

$$1 = f_S + f_M + f_A \tag{1}$$

$$\text{Sal} = f_S \times \text{Sal}_S + f_M \times \text{Sal}_M + f_A \times \text{Sal}_A \tag{2}$$

where f and Sal are the abbreviations for fraction and salinity, respectively. On the left hand side of Eq. (2), Sal is the measured salinity value at a specific station. On the right hand side of Eqs. (1) and (2), the subscripts S, M and A designate the endmembers of seawater, and the Mississippi and the Atchafalaya rivers, respectively, which are listed in Table 1.

Similarly, the TA value due to conservative mixing (C_{mix}) is the fractional sum of TA from the various endmembers (TA values of C_S, C_A, and C_M in Table 1)

$$C_{mix} = f_S \times C_S + f_M \times C_M + f_A \times C_A \tag{3}$$

Analogous relationships and corresponding endmembers can be applied for other species: DIC, NO_3, PO_4^{3-} and $Si(OH)_4$. We then can estimate the difference between the observed concentration of an element (C) and its predicted conservative concentration (C_{mix}) as the biological drawdown or addition (ΔC) $\Delta C = C_{mix} - C$, of DIC (ΔDIC), nitrate (ΔNO_3), phosphate (ΔPO_4) and $Si(OH)_4$ (ΔSi).

To determine the value of the three unknown fractional terms in addition to Eqs. (1) and (2), we use the TA balance as the third mass conservation equation. TA will increase by one unit for every one unit decrease resulting from the biological drawdown of NO_3, $\Delta TA = -\Delta NO_3$ (Brewer and Goldman, 1976; Wolf-Gladrow et al., 2007). However, it is important to recognize that in coastal waters, particularly in estuarine or river plume waters, NO_3 concentration changes associated with water mass mixing do not contribute to TA. Thus a combination of the conservative mixing value and the biological drawdown of TA can be expressed as:

$$TA = f_S \times TA_S + f_M \times TA_M + f_A \times TA_A + \Delta NO_3 \tag{4}$$

Based on Eq. (3) the biological drawdown of ΔNO_3 can be expressed as:

$$\Delta NO_3 = C_{mix} - C = f_S \times NO_{3S} + f_M \times NO_{3M} + f_A \times NO_{3A} - NO_3 \tag{5}$$

By replacing the ΔNO_3 in Eq. (4) by Eq. (5), we have

$$TA + NO_3 = f_S \times (TA_S + NO_{3S}) + f_M \times (TA_M + NO_{3M}) + f_A \times (TA_A + NO_{3A}) \tag{6}$$

Therefore, we can infer that the so-called potential alkalinity, ($TA + NO_3$) is a conservative tracer in addition to salinity (Bates et al., 1998; Brewer and Goldman, 1976). Thus, for any paired observations of Sal_i and $(TA + NO_3)_i$, we can derive f_{Si}, f_{Mi}, and f_{Ai} by Eqs. (1), (2) and (6); and derive C_{mix} and ΔC for other species thereafter.

Uptake ratios of carbon and nutrients in a large river plume

W.-J. Huang et al.

Full Screen / Esc

Printer-friendly Version

Interactive Discussion

In June 2003, our study area was close to the Mississippi River mouth. The different increasing rates of riverine TA value suggested that the Mississippi River endmember was more stable in June 2003 (1.7–3.4 μM d^{-1}) than in August 2004 (6.4–10 μM d^{-1}). As will be discussed in Sect. 3.1, it is appropriate to use a two-endmember model in this case. A two-endmember mixing is a special case of the three-endmember mixing when one of the endmembers can be neglected or the two endmembers have similar property values. Therefore, C_{mix} and ΔC in June 2003 can be solved by setting f_A as zero in Eqs. (1), (2), and (6). For the multi-endmember mixing case, a non-negative solver function (Lawson and Hanson, 1974) in the Matlab$^{®}$ software package was adapted to solve the least square equation with the constraint to exclude solutions with negative values of the fractions. Because there were uncertainties in both "x" and "y" variables a Type II linear regression, the major axis method (York, 1966) was used to calculate the slopes of ΔDIC to ΔNO$_3$, ΔDIC to ΔPO$_4$, and ΔDIC to ΔSi.

3 Result and discussion

3.1 Mixing schemes based on salinity and total alkalinity

Patterns of salinity distribution and TA distribution were used to examine the mixing processes between freshwater and seawater in the Mississippi River plume. For June 2003, there was a strong salinity gradient across the Louisiana Bight attributable to Mississippi River discharge and the coastal circulation patterns (Fig. 2a). Salinity was lower closer to land and towards the northeast and higher towards the southwest. The TA distribution (Fig. 2b) was very similar to salinity distribution, consistent with a dominating influence by the Mississippi River in the region studied. As such we used a two endmember mixing model – Mississippi River and seawater. This two endmember mixing model is robust because of the strong correlation between TA and salinity for this period and region of study (Fig. 2c). The river endmember was also relatively stable as the river endmember TA value increased only from 1.7–3.4 μM d^{-1} during 12 May– 24 June 2003 prior to the June 2003 cruise (Fig. 1).

The salinity pattern was quite different in August 2004 with low values confined to the area immediately adjacent to Southwest Pass and approaching the Atchafalaya Bay (Fig. 2d). Salinity increased with distance from these riverine freshwater sources. Distributions of TA were characterized by higher values close to Southwest Pass and the Atchafalaya Bay (Fig. 2e). An examination of TA versus salinity relationships revealed multiple endmembers with strong contributions from the Mississippi, Atchafalaya and seawater for this period (Fig. 2f). A three-endmember mixing model was therefore applied to data for salinities greater than 24 for this dataset. In addition, as the riverine endmember TA values were increasing rapidly during the period before the cruise (6.4–10 μM d^{-1}), it was necessary to adjust endmember values to account for this increase. Therefore, as the freshwater transit times were on the order of 8–10 days to reach a salinity range of 24–32 (Green et al., 2006), we chose river TA values as the endmembers 8 and 10 days before the cruise for the Mississippi and Atchafalaya rivers (Table 1). The uncertainties induced by the water transit time were considered in Sect. 3.4. By applying these appropriate river endmember values (USGS data, Table 1), the TA values for salinities greater than 24 were generally within the three-endmember mixing trajectory and thus were taken to be conservative (Fig. 2f). On the other hand, high TA values for salinities less than 24 were likely the result of the dramatic increase in the river endmember TA in the days prior to the cruise (Fig. 2f).

3.2 Relationships of DIC and nutrient concentrations and biological removal to location

DIC and nutrients in both seasons showed non-linear relationships with salinity (Fig. 3), which are consistent with previous studies (Cai, 2003; Dagg et al., 2007). For the June 2003 dataset, maximum biological nutrient and DIC uptake were observed at salinities between 10 and 16 (Fig. 3a). This pattern differs from observations made for more than a dozen other cruises between 2003 and 2011, where maximum biological removal was observed at salinities above 18 (Cai, 2003; W.-J. Cai, unpublished data). This early removal was possibly due to a bloom seeded by freshwater diatoms (Dagg

et al., 2008). The DIC values in August 2004 also deviated greatly from the mixing lines (Fig. 3c). Similar non-conservative trends were evident in nutrient verses salinity plots (Fig. 3c,d). In addition, NO_3 concentrations were lower than that of $Si(OH)_4$ for samples corresponding to maximum biological removal of DIC, especially in June 2003 (Fig. 3b). This will be addressed in a later section. As DIC and nutrient values were affected by both mixing and biological uptake, the two-endmember model was applied for June 2003 and the three-endmember model for August 2004 to quantify the magnitude and stoichiometry of net uptake. Furthermore, we also examined the relationships of DIC and nutrients to their corresponding sample locations to identify the regional differences.

Relationships among DIC, TA and nutrients differed depending on salinity, strength of biological removal, and sampling location. For example, in June 2003, for stations with surface salinities less than 24 (Northeastern Louisiana Bight, Fig. 4), TA, NO_3, PO_4^{3-} and $Si(OH)_4$ concentrations which deviated from the conservative mixing line and approached the Redfield-type uptake line (Fig. 4a–d) had strong biological removals (ΔC in Fig. 4f–h). In addition, the salinity regions corresponding to strong removal DIC and nutrients coincided with high Chl-*a* and DOC concentrations, consistent with high biological production as reported previously (Dagg et al., 2008). In contrast, in the Southwestern Louisiana Bight (Fig. 4 blue squares), where salinities were greater than 24, concentrations of NO_3, PO_4^{3-} and $Si(OH)_4$ were closer to the conservative mixing line (Fig. 4a–d) and thus less influenced by biological removal (Fig. 4f–h).

In August 2004, as the Louisiana Bight was generally characterized by salinities greater than 24 waters (red and blue squares in Fig. 5), net uptake of all elements was less than that observed in June 2003, suggesting less intense biological production. For low salinity waters proximal to the river mouth, nutrient data were lacking and so it was not possible to calculate net uptake or stoichiometry.

Uptake ratios of carbon and nutrients in a large river plume

W.-J. Huang et al.

3.3 Stoichiometry

In considering the stoichiometric uptake of DIC and nutrients, it is important to recognize that DIC uptake and nutrient removal as determined in this study (i.e., by subtracting concentrations estimated for conservative mixing alone) reflect the net effect of autotrophy plus heterotrophy. The concept of varying source terms that differ in stoichiometry was reported by Frigstad et al. (2011), who found that the average C/N ratio of suspended particulate organic material (POM) in the Norwegian shelf was the combined result of C : nutrient ratios of autotrophs that were generally lower than Redfield and ratios of non-autotrophs that were above or close to Redfield value. Different contributions to the net biological removal by distinct sources terms may explain observed temporal and spatial differences in stoichiometry (Pahlow and Riebesell, 2000; Li et al., 2000; Li and Peng, 2002). For example, C/N remineralization ratios of 5.48 were reported in the Atlantic Ocean (Li et al., 2000) compared to 4.6 ± 0.6 between latitudes $45°$ N–$5°$ N (Li and Peng, 2002). Despite the fact that several factors can affect the $\Delta DIC : \Delta NO_3$ relationships, it is notable that results reported for this study (Table 2) were surprisingly close to the Redfield C/N ratio and comparable to previously reported remineralization values. This result implies that net effect of autotrophy and heterotrophy on biological uptake stoichiometry was close to the Redfield ratio in the Mississippi River plume.

We observed large deviations from the Redfield ratio for $\Delta DIC : \Delta PO_4$ and $\Delta DIC : \Delta Si$ (Table 2). Higher slopes of ΔDIC to ΔPO_4 could have resulted from utilization of organic phosphorus, an argument supported by observations of high alkaline phosphatase activities in the plume (Ammerman and Glover, 2000; Sylvan et al., 2007) and could also be attributed to preferential PO_4^{3-} release relative to C from suspended particulates (Chambers et al., 1995). These two explanations were also probable reasons for the relatively high PO_4^{3-} concentration (3.6 µM) measured at the station ~ 30 km south of the Mississippi River channel in August 2004. Since this value was higher than the endmembers, this value was not included in the ΔPO_4 calculation. We noticed that

slopes of ΔDIC to ΔPO_4 differed substantially between these two cruises and this may due to differences in relative rates of remineralization and uptake during the two cruises, likely attributable to physiological differences between and within autotrophic and heterotrophic fractions of the microbial populations during these two cruises (for example, as was recently reported in the Norwegian shelf, Frigstad et al., 2011). Given the potential contributions by other source terms to observed PO_4^{3-} and preferential remineralization of P relative to C, it is acknowledged that using riverine phosphate input to estimate the carbon uptake in the plume area may result in a bias. Carbon and silicate uptake varied greatly between these two cruises, but this is to be expected with variations in phytoplankton community structure likely to occur during spring to summer conditions and with decreased productivity. We found that the slope of ΔDIC versus ΔSi relationship in August 2004 (4.1 ± 0.8) was different from that in June 2003 (11.2 ± 1.1, Table 2) and also noticed that the slope of ΔSi versus ΔNO_3 was 0.50 ± 0.1 in June 2003 and was 1.2 ± 0.4 in August 2004 (Table 2). Further explanations for the differences in the slopes of ΔDIC versus ΔSi, and ΔSi versus ΔNO_3 are discussed in Sect. 3.6.

3.4 Impacts of river endmembers and plume transit time on stoichiometry assessments

The uncertainties of the multiple-endmember model depend on the accuracy of estimates of river endmembers and plume water transit time, the latter of which depends on the river discharge, tide, wind, and coastal currents (Walker et al., 2005). Plume water transit time was estimated as two days for salinities in the range of 0–13, two days for salinities of 13–24, six days for salinities of 24–32, and six days for salinities of 32–34.5 based on satellite-derived suspended sediment distributions collected during 1989–1997 (Green et al., 2006). The uncertainties of water residence times propagate to the uncertainties in the river endmember. Additionally, the relationship between nutrient concentrations and river flow differs from nutrient to nutrient. TA values increase with decreasing discharge (Cai et al., 2008) in the Mississippi (Cai 2003, Fig. 1)

and Atchafalaya rivers: with decreasing discharge during our study we observed TA increases of 1.7 to 3.4 μM d^{-1} before the first cruise (increasing 74 to 132 μM during 12 May–24 June 2003) and average 6.4 to 10 μM d^{-1} before the second cruise (increasing 382 μM during 22 June–9 August 2004, $\sim$ 200 μM in the last 20 days, Fig. 1). If we assume an uncertainty of 1 day for the water transit time, this leads to a propagated uncertainty in TA of 4–14 μM for the river endmembers, assuming the TA river endmember increases 2–7 μM d^{-1}. Phosphate concentrations in the Mississippi River (Lohrenz et al., 1999) have been reported to slightly increase with decreasing discharge (0.1 μM over the same period) while nitrate and silicate concentrations were found to decrease ($\sim$ 0.6, $\sim$ 1 μM d^{-1}, respectively). Therefore, variations in discharge will contribute to uncertainties in net uptake stoichiometry that will depend on the direction of change in discharge and the type of nutrient considered. Despite these uncertainties, we argue that our estimates of biological removal are robust because first, the river endmember was relatively stable in June 2003, reflected by the good linear correlation between salinity and TA, and second, the 10 % of the variation in the river endmember in August 2004 resulted in only a 0.1 % change in estimated values for salinities larger than 24.

3.5 Rates of biological removal

We calculated biological removal rates by dividing DIC removal by the plume water transit time (Cai, 2003). Here, transit times were estimated by using the freshwater residence times reported by Green et al. (2006) as described in Sect. 3.4. In June 2003, nonconservative uptake deviations for ΔDIC were 10–450 μM for salinities less than 24 and were less than 130 μM for salinities greater than 24. The corresponding rates of DIC removals were 0.6–1.3 gC m^{-3} d^{-1} and 0–0.15 gC m^{-3} d^{-1}, respectively (5–108 μmol l^{-1} d^{-1} and 0–13 μmol l^{-1} d^{-1} over 4 or 10–16 days, respectively). In August 2004, DIC removal rates were 0.1–0.19 gC m^{-3} d^{-1} for surface salinities greater than 24. These DIC removal rates were comparable to those reported by Cai (2003) of 1–2 gC m^{-3} d^{-1} for August and September 1998. Similarly, primary production rates estimated by the ^{14}C incubation method in April 1988 were 1 to 5 gC m^{-3} d^{-1} in the

salinity range of 15–36 (Lohrenz et al., 1990), again consistent with our estimates of DIC removal. Green et al. (2006) used a biological model to estimate DIC removal rates in summer of 0.102, 0.818, 0.491, and 0.120 gC m^{-3} d^{-1} for salinity ranges of 0–18, 18–24, 24–32, 32–34.5, respectively. Our estimates of DIC removal rates were slightly higher than those estimated by Green et al. (2006) for the low to mid salinity range and were comparable for the high salinity range (i.e., greater than 24). The plume appeared to be very productive in June 2003 (cf. Dagg et al., 2008), which may explain our higher observed rates at low to mid-salinities. As the uncertainties mentioned in Sect. 3.4 also affect the estimated biological removals results, we have more confidence in the mid- to high salinity biological removals because of less sensitivity to the water transit uncertainties. Despite the larger water transit time uncertainties for our estimates of biological removals at low salinities, our estimated removal rates were still on the same order of magnitude as previous studies.

3.6 Silicate removal and Si-N relationship

Correlations of ΔDIC/ΔNO$_3$ were fairly high ($R^2 > 0.745$) but the correlations of ΔDIC/ΔSi were much lower ($R^2 < 0.443$) in Table 2. To further explore the weak correlations between ΔDIC and ΔSi, we therefore compared the observed values of Si(OH)$_4$ and NO$_3$ in relationship to sampling locations. We found that the relationships between Si(OH)$_4$ and NO$_3$ were strongly dependent on location (Fig. 6a,b) which was consistent with the observed variations in relationships between DIC and nutrients as described in Sect. 3.2 (Figs. 4 and 5). For example, a relationship of high silicate concentration ($> 2\,\mu$M) relative to low nitrate concentration ($< 10 \sim 11\,\mu$M, hereafter referred to as HSiLN) was observed for the Northeast Louisiana Bight in June 2003 (Fig. 6a, 4e), while low concentrations of silicate and nitrate (hereafter referred to as LSiLN) were found in the Southwestern Louisiana Bight (Fig. 6a, 4e). A similar spatial dependency in nutrient relationships was observed in August 2004 (Figs. 6b and 5e). If we only consider the LSiLN area with salinities greater than 24 (Fig. 6c,d), the slope of the ΔSi versus ΔNO$_3$ relationship was 0.7 ± 0.1 in June 2003 and was 1.1 ± 0.2 in August

2004. These slopes were comparable to relationships reported in a previous study (0.8, Fisher et al., 1988) and close to the Redfield Si/N ratio of one (Redfield, 1958; Brzezinski, 1985).

Because ΔSi was lower than expected if removal were due to equivalent uptake of both silicate and nitrate, such as uptake of diatom community (Brzezinski, 1985), we inferred an additional source term for silicate or a preferential removal of nitrogen over silicate (Fig. 6c,d). The marshes and bays along the Louisiana coast could be significant sources of dissolved Si (Struyf et al., 2006), and we considered this possibility by examining patterns in Si concentrations in relationship to proximity to Barataria Bay.

3.7 The role of salt marshes and bays

We found that waters close to Barataria Bay had very high Si concentrations, especially in June 2003 (Figs. 4 and 5), and speculate that this was due to net export from the Barataria Bay, a phenomenon that might be expected for a coastal ecosystem experiencing wetland loss (Ren et al., 2009). In the same cruise, Dagg et al. (2008) also found that POC, PON, Chl-*a*, and TSM (total suspended material) were high in the Northern Louisiana Bight and argued that the particulate material was representative of output from the Barataria Bay, consistent with physical characterizations of exchange processes in this system (Li et al., 2011). In addition, low diatom abundance was observed at locations coinciding with our HSiLN stations during the same cruise in 2003 (Dagg et al., 2008). This was consistent with a reduced utilization of Si by a non-diatom dominated populations, but may also reflect a preferentially high source term for Si from the marsh. Therefore, the degree to which elemental stoichiometry might reflect inputs from the extensive intertidal marshes needs further investigation. Our results still support the use of riverine Si input for estimation of DIC drawdown in the river plume, provided that areas near marshes and bays are excluded from the analysis.

4   Summary and implication

To conclude, the biogeochemical processes in the Mississippi River plume and the adjacent coastal waters exhibited considerable spatial heterogeneity, with evidence of strong biological removal of carbon and nutrients in mid-salinity waters. The later is especially true in June 2003. Relationships between DIC and nutrients were strongly dependent on salinity range and geographic location, and influenced by biological removal. Localized inputs of freshwater and possible inputs from marshes adjacent to the Louisiana Bight were contributing factors in the observed patterns.

We examined net uptake stoichiometry of DIC and nutrients and how well it conforms to the to Redfield ratios. The stoichiometry of carbon and nutrient removal in the Mississippi River plume was affected by multiple biogeochemical processes. Slopes of ΔDIC versus ΔNO_3 were largely dominated by net biological removal. Slopes of ΔDIC versus ΔPO_4 relationship were also likely affected by additional source terms for PO_4^{3-} including remineralization of organic forms of P, possible release from suspended particulates (Chambers et al., 1995). Slopes of the ΔDIC versus ΔSi relationship were apparently influenced by a combination of localized inputs from adjacent wetlands and uptake by phytoplankton. Therefore, provided that localized non-Redfield inputs of Si are excluded from analysis, our results show general agreement with Redfield-type C/N/Si ratios for predicting the net uptake relationships of DIC to inorganic N and Si. These findings have implications for applications to biogeochemical models of large river plumes.

References

Anderson, L. A. and Sarmiento, J. L.: Redfield ratios of remineralization determined by nutrient data analysis, Global Biogeochem. Cy., 8, 65–80, doi:10.1029/93gb03318, 1994.

Ammerman, J. W. and Glover, W. B.: Continuous underway measurement of microbial ectoenzyme activities in aquatic ecosystems, Mar. Ecol.-Prog. Ser., 201, 1–12, doi:10.3354/meps201001, 2000.

Bates, N. R., Hansell, D. A., Carlson, C. A., and Gordon, L. I.: Distribution of CO_2 species, estimates of net community production, and air-sea CO_2 exchange in the Ross Sea polynya, J. Geophys. Res., 103, 2883–2896, doi:10.1029/97jc02473, 1998.

Borges, A. V. and Gypens, N.: Carbonate chemistry in the coastal zone responds more strongly to eutrophication than to ocean acidification, Limnol. Oceanogr., 55, 346–353, 2010.

Brewer, P. G. and Goldman, J. C.: Alkalinity changes generated by phytoplankton growth, Limnol. Oceanogr., 21, 108–117, 1976.

Brzezinski, M. A.: The Si : C : N ratio of marine diatoms: interspecific variability and the effect of some environmental variables, J. Phycol., 21, 347–357, 1985.

Cai, W.-J.: Riverine inorganic carbon flux and rate of biological uptake in the Mississippi River plume, Geophys. Res. Lett., 30, 1032, doi:10.1029/2002GL016312, 2003.

Cai, W.-J. and Wang, Y.: The chemistry, fluxes, and sources of carbon dioxide in the estuarine waters of the Satilla and Altamaha rivers, Georgia, Limnol. Oceanogr., 43, 657–668, 1998.

Cai, W.-J., Guo, X., Chen, C.-T. A., Dai, M., Zhang, L., Zhai, W., Lohrenz, S. E., Yin, K., Harrison, P. J., and Wang, Y.: A comparative overview of weathering intensity and HCO_3^- flux in the world's major rivers with emphasis on the Changjiang, Huanghe, Zhujiang (Pearl) and Mississippi rivers, Cont. Shelf Res., 28, 1538–1549, 2008.

Cai, W.-J., Hu, X., Huang, W.-J., Jiang, L.-Q., Wang, Y., Peng, T.-H., and Zhang, X.: Alkalinity distribution in the Western North Atlantic Ocean margins, J. Geophys. Res., 115, C08014, doi:10.1029/2009jc005482, 2010.

Chambers, R., Fourqurean, J., Hollibaugh, J., and Vink, S.: Importance of terrestrially-derived, particulate phosphorus to phosphorus dynamics in a west coast estuary, Estuaries Coasts, 18, 518–526, doi:10.2307/1352369, 1995.

Dagg, M., Bianchi, T., Breed, G., Cai, W., Duan, S., Liu, H., McKee, B., Powell, R., and Stewart, C.: Biogeochemical characteristics of the lower Mississippi River, USA, during June 2003, Estuaries Coasts, 28, 664–674, 2005.

Uptake ratios of carbon and nutrients in a large river plume

W.-J. Huang et al.

Title Page

Abstract	Introduction
Conclusions	References
Tables	Figures

◄ ► ► I

◄ ►

Back | Close

Full Screen / Esc

Printer-friendly Version

Interactive Discussion

Dagg, M., Ammerman, J., Amon, R., Gardner, W., Green, R., and Lohrenz, S.: A review of water column processes influencing hypoxia in the Northern Gulf of Mexico, Estuaries Coasts, 30, 735–752, 2007.

Dagg, M. J., Bianchi, T., McKee, B., and Powell, R.: Fates of dissolved and particulate materials from the Mississippi River immediately after discharge into the Northern Gulf of Mexico, USA, during a period of low wind stress, Cont. Shelf Res., 28, 1443–1450, 2008.

Das, A., Justic, D., and Swenson, E.: Modeling estuarine-shelf exchanges in a deltaic estuary: implications for coastal carbon budgets and hypoxia, Ecol. Model., 221, 978–985, 2010.

DeMaster, D. J. and Pope, R. H.: Nutrient dynamics in Amazon shelf waters: results from AMASSEDS, Cont. Shelf Res., 16, 263–289, 1996.

Donald, K. M., Joint, I., Rees, A. P., Malcolm, S., Woodward, E., and Savidge, G.: Uptake of carbon, nitrogen and phosphorus by phytoplankton along the 20° W meridian in the ne atlantic between 57.5° N and 37° N, Deep-Sea Res. Pt. II, 48, 873–897, doi:10.1016/s0967-0645(00)00102-8, 2001.

Fennel, K., Hetland, R., Feng, Y., and DiMarco, S.: A coupled physical-biological model of the Northern Gulf of Mexico shelf: model description, validation and analysis of phytoplankton variability, Biogeosciences, 8, 1881–1899, doi:10.5194/bg-8-1881-2011, 2011.

Fisher, T. R., Harding, L. W., Stanley, D. W., and Ward, L. G.: Phytoplankton, nutrients, and turbidity in the Chesapeake, Delaware, and Hudson estuaries, Estuar. Coast. Shelf S., 27, 61–93, 1988.

Frigstad, H., Andersen, T., Hessen, D. O., Naustvoll, L.-J., Johnsen, T. M., and Bellerby, R. G. J.: Seasonal variation in marine $C : N : P$ stoichiometry: can the composition of seston explain stable Redfield ratios?, Biogeosciences, 8, 2917–2933, doi:10.5194/bg-8-2917-2011, 2011.

Gazeau, F., Gattuso, J.-P., Middelburg, J., Brion, N., Schiettecatte, L.-S., Frankignoulle, M., and Borges, A.: Planktonic and whole system metabolism in a nutrient-rich estuary (the scheldt estuary), Estuaries Coasts, 28, 868–883, doi:10.1007/bf02696016, 2005.

Geider, R. and La Roche, J.: Redfield revisited: Variability of $C : N : P$ in marine microalgae and its biochemical basis, Eur. J. Phycol., 37, 1–17, doi:10.1017/s0967026201003456, 2002.

Green, R. E., Bianchi, T. S., Dagg, M. J., Walker, N. D., and Breed, G. A.: An organic carbon budget for the Mississippi River turbidity plume and plume contributions to air-sea CO_2 fluxes and bottom water hypoxia, Estuaries Coasts, 29, 579–597, doi:10.1007/BF02784284, 2006.

Green, R. E., Breed, G. A., Dagg, M. J., and Lohrenz, S. E.: Modeling the response of primary

production and sedimetation to variable nitrate loading in the Mississippi River plume, Cont. Shelf Res., 28, 1451–1465, 2008.

Gypens, N., Lancelot, C., and Borges, A. V.: Carbon dynamics and CO_2 air-sea exchanges in the eutrophied coastal waters of the Southern Bight of the North Sea: a modelling study, Biogeosciences, 1, 147–157, doi:10.5194/bg-1-147-2004, 2004.

Hecky, R. E., Campbell, P., and Hendzel, L. L.: The stoichiometry of carbon, nitrogen, and phosphorus in particulate matter of lakes and oceans, Limnol. Oceanogr., 38, 709–724 1993.

van Heerden, I. L., Wells, J. T., and Roberts, H. H.: River-dominated suspended-sediment deposition in a new Mississippi Delta, Can. J. Fish. Aquat. Sci., 40(S1), 60–71, 1983.

Hopkinson, C. S. and Vallino, J. J.: Efficient export of carbon to the deep ocean through dissolved organic matter, Nature, 433, 142–145, 2005.

Hupe, A. and Karstensen, J.: Redfield stoichiometry in Arabian Sea subsurface waters, Global Biogeochem. Cy., 14, 357–372, doi:10.1029/1999gb900077, 2000.

Lawson, C. L. and Hanson, R. J.: Solving Least Squares Problems, Prentice-Hall, Chapter 23, 161 pp., 1974.

Li, C., White, J. R., Chen, C., Lin, H., Weeks, E., Galvan, K., and Bargu, S.: Summertime tidal flushing of Barataria Bay: transports of water and suspended sediments, J. Geophys. Res., 116, C04009, doi:10.1029/2010jc006566, 2011.

Li, Y.-H. and Peng, T.-H.: Latitudinal change of remineralization ratios in the oceans and its implication for nutrient cycles, Global Biogeochem. Cy., 16, 1130, doi:10.1029/2001gb001828, 2002.

Li, Y.-H., Karl, D. M., Winn, C. D., Mackenzie, F. T., and Gans, K.: Remineralization ratios in the subtropical North Pacific gyre, Aquat. Geochem., 6, 65–85, 2000.

Lohrenz, S. E., Dagg, M. J., and Whitledge, T. E.: Enhanced primary production at the plume/oceanic interface of the Mississippi River, Cont. Shelf Res., 10, 639–664, 1990.

Lohrenz, S. E., Fahnenstiel, G. L., Redalje, D. G., Lang, G. A., Chen, X., and Dagg, M. J.: Variations in primary production of Northern Gulf of Mexico continental shelf waters linked to nutrient inputs from the Mississippi River, Mar. Ecol.-Prog. Ser., 155, 45–54, doi:10.3354/meps155045, 1997.

Lohrenz, S. E., Fahnenstiel, G. L., Redalje, D. G., Lang, G. A., Dagg, M. J., Whitledge, T. E., and Dortch, Q.: Nutrients, irradiance, and mixing as factors regulating primary production in coastal waters impacted by the Mississippi River plume, Cont. Shelf Res., 19, 1113–1141, 1999.

Uptake ratios of carbon and nutrients in a large river plume

W.-J. Huang et al.

Morey, S. L., Martin, P. J., O'Brien, J. J., Wallcraft, A. A., and Zavala-Hidalgo, J.: Export pathways for river discharged fresh water in the Northern Gulf of Mexico, J. Geophys. Res., 108, 3303, doi:10.1029/2002jc001674, 2003.

Pahlow, M. and Riebesell, U.: Temporal trends in deep ocean redfield ratios, Science, 287, 831–833, doi:10.1126/science.287.5454.831, 2000.

Redfield, A. C.: The biological control of chemical factors in the environment, Am. Sci., 46, 205–221, 1958.

Ren, L., Rabalais, N. N., Turner, R. E., Morrison, W., and Mendenhall, W.: Nutrient limitation on phytoplankton growth in the upper Barataria Basin, Louisiana: microcosm bioassays, Estuaries Coasts, 32, 958–974, 2009.

Seitzinger, S. P. and Sanders, R. W.: Contribution of dissolved organic nitrogen from rivers to estuarine eutrophication, Mar. Ecol.-Prog. Ser., 159, 1–12, doi:10.3354/meps159001, 1997.

Seitzinger, S. P., Sanders, R. W., and Styles, R.: Bioavailability of don from natural and anthropogenic sources to estuarine plankton, Limnol. Oceanogr., 47, 353–366, 2002.

Struyf, E., Dausse, A., Van Damme, S., Bal, K., Gribsholt, B., Boschker, H. T. S., Middelburg, J. J., and Meire, P.: Tidal marshes and biogenic silica recycling at the land-sea interface, Limnol. Oceanogr., 51, 838–846, 2006.

Sylvan, J. B., Quigg, A., Tozzi, S., and Ammerman, J. W.: Eutrophication-induced phosphorus limitation in the Mississippi River plume: evidence from fast repetition rate fluorometry, Limnol. Oceanogr., 52, 2679–2685, 2007.

Takahashi, T., Broecker, W. S., and Langer, S.: Redfield ratio based on chemical data from isopycnal surfaces, J. Geophys. Res., 90, 6907–6924, doi:10.1029/JC090iC04p06907, 1985.

Ternon, J. F., Oudot, C., Dessier, A., and Diverres, D.: A seasonal tropical sink for atmospheric CO_2 in the Atlantic Ocean: the role of the Amazon River discharge, Mar. Chem., 68, 183–201, 2000.

Turner, R. E., Qureshi, N., Rabalais, N. N., Dortch, Q., Justic, D., Shaw, R. F., and Cope, J.: Fluctuating silicate:nitrate ratios and coastal plankton food webs, P. Natl. Acad. Sci. USA, 95, 13048–13051, 1998.

Walker, N. D., Wiseman, W. J., Rouse, L. J., and Babin, A.: Effects of river discharge, wind stress, and slope eddies on circulation and the satellite-observed structure of the Mississippi River plume, J. Coastal Res., 21, 1228–1244, doi:10.2112/04-0347.1, 2005.

Wolf-Gladrow, D. A., Zeebe, R. E., Klaas, C., Körtzinger, A., and Dickson, A. G.: Total alkalinity:

Title Page

Abstract | Introduction

Conclusions | References

Tables | Figures

◄ | ►►

◄ | ►

Back | Close

Full Screen / Esc

Printer-friendly Version

Interactive Discussion

the explicit conservative expression and its application to biogeochemical processes, Mar. Chem., 106, 287–300, 2007.

York, D.: Least-squares fitting of a straight line, Can. J. Phys., 44(5), 1079–1086, doi:10.1139/p66-090, 1966.

Zimmerman, R. J., Minello, T. J., and Rozas, L. P.: Salt marsh linkages to productivity of penaeid shrimps and blue crabs in the Northern Gulf of Mexico, in: Concepts and Controversies in Tidal Marsh Ecology, edited by: Weinstein, M. P. and Kreeger, D. A., Springer Netherlands, 293–314, 2002.

Uptake ratios of carbon and nutrients in a large river plume

W.-J. Huang et al.

Title Page

Abstract | Introduction

Conclusions | References

Tables | Figures

◄ | ►

◄ | ►

Back | Close

Full Screen / Esc

Printer-friendly Version

Interactive Discussion

W.-J. Huang et al.

Table 1. Endmembers of the Mississippi River (C_M), the Atchafalaya River (C_A), and marine end (C_S) for DIC, TA and nutrients values in June 2003 and August 2004. Unit: µmol l^{-1}, except salinity.

Season	Endmember	Salinity	TA	DIC	NO_3	PO_4^{3-}	$Si(OH)_4$
Jun 2003	C_M	0[1]	2032[1]	2051[1]	114.9[1]	2.0[1]	97.8[1]
Jun 2003	C_S	33.5[6]	2422.5[6]	2068[6]	0.4[6]	0.7[6]	1.6[6]
Aug 2004	C_A	0.1[2]	1679[2]	1729[3]	72.1[2]	2.4[2]	103.9[2]
Aug 2004	C_M	0.1[4]	2200[4]	2266[3]	107.1[4]	3.1[4]	104.1[4]
Aug 2004	C_M	1.6[5]	2502.8[5]	2488.3[5]	149[5]	1.2[5]	85[5]
Aug 2004	C_S	35.8[6]	2502.7[6]	2119.3[6]	1.2[6]	1.1[6]	1.8[6]

[1] Cited from the lower Mississippi River cruise (Dagg et al., 2005).

[2] TA, PO_4^{3-} and $Si(OH)_4$ were modeled by discharge (Q) to species' flux relationship (concentration × Q) and NO_3 was modeled by nitrate to nitrate flux relationship in 2004 based on the Q on 7/28. Q was adapted from USGS site, Morgan City (site# 07381600) and species concentrations were adapted from at USGS site, Melville (site# 07381495).

[3] Use an empirical equation DIC = 1.03 × TA in the Atchafalaya River and the Mississippi River based on 2008–2010 measurements (W.-J. Cai, unpublished data).

[4] Average observations on 20 July 2004 and 17 August 2004 at USGS site, Belle Chase (site# 07374525).

[5] This Mississippi River endmember was measured during the cruise in the river channel and was listed here for comparison. This endmember was not used for ΔC calculation as we believe that the true endmember has been variable with time.

[6] Sea endmember were measured during the cruise.

Table 2. Stoichiometry of DIC uptake and nutrient removals and their correlation coefficients (R^2).

	$\Delta DIC/\Delta NO_3$	$\Delta DIC/\Delta PO_4$	$\Delta DIC/\Delta Si$	$\Delta Si/\Delta NO_3$	$\Delta NO_3/\Delta PO_4$	C/Si/N/P
June 2003	5.7 ± 0.3	281.9 ± 21.3	11.2 ± 1.1	0.5 ± 0.1	49.8 ± 2.9	90.7/ 8.1/ 16/ 0.3
R^2	0.745	0.621	0.416	0.588	0.773	
August 2004	5.0 ± 1.1	135.3 ± 18.6	4.1 ± 0.8	1.2 ± 0.4	25.9 ± 4.4	79.5/ 20.0/ 16/ 0.6
R^2	0.875	0.578	0.443	0.733	0.644	
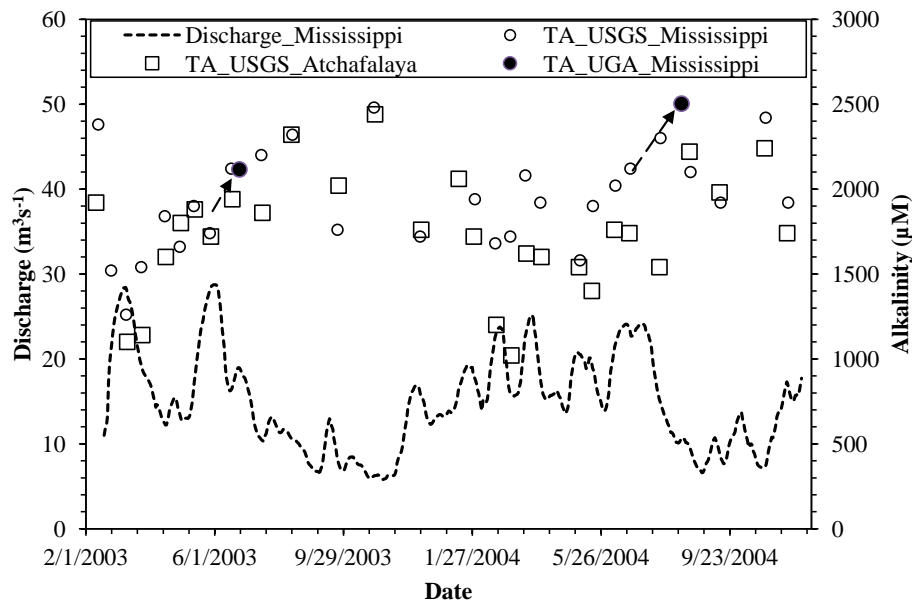
Fig. 1. Temporal variation of the discharge and TA. The open circles are the TA values at the USGS site, St. Francisville (site# 07373420). Solid circles are the TA concentrations measured in the Mississippi River channel in this study. Dashed line is the daily discharge data from USGS site, St. Francisville. Square symbols represent the TA values in the Atchafalaya River at USGS site Melville (#07381495). The two dashed arrows indicate the increasing rate of TA prior to the cruise periods: $1.7\,\mu M\,d^{-1}$ during 12 May–24 June 2003 (increasing $75\,\mu M$) and $6.4\,\mu M\,d^{-1}$ during 22 June–11 August 2004 (increasing $322\,\mu M$).
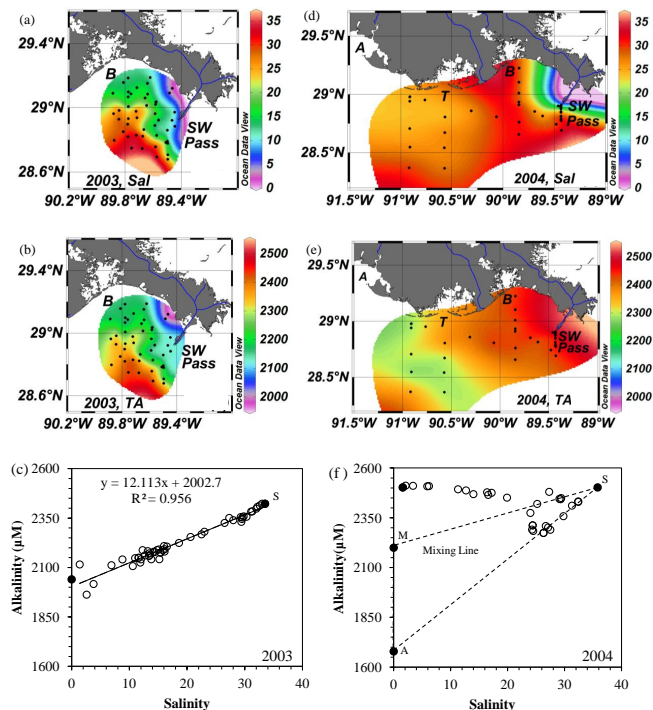
Fig. 2. Salinity and TA distributions, and TA versus salinity relationships. Penal **(a)** and **(b)** are the salinity and TA distribution in June 2003, respectively; panel **(d)** and **(e)** show the salinity and TA distribution in August 2004, respectively. "A" represents the Atchafalaya Bay, "T" is the Terrebonne Bay, "B" is the Barataria Bay, "SW Pass" is the Southwest Pass of the Mississippi River. Black dots in the spatial distribution are the sampling sites. Panel **(c)** and **(f)** show the relationship between salinity and TA in June 2003 and August 2004, respectively, where black circles are the endmembers. The solid line represents the linear regression line in panel **(c)**. "M", "A", and "S" represent endmembers of the Mississippi River, the Atchafalaya River, and seawater in panel **(f)**, respectively. The dash line represents the conservative mixing line.
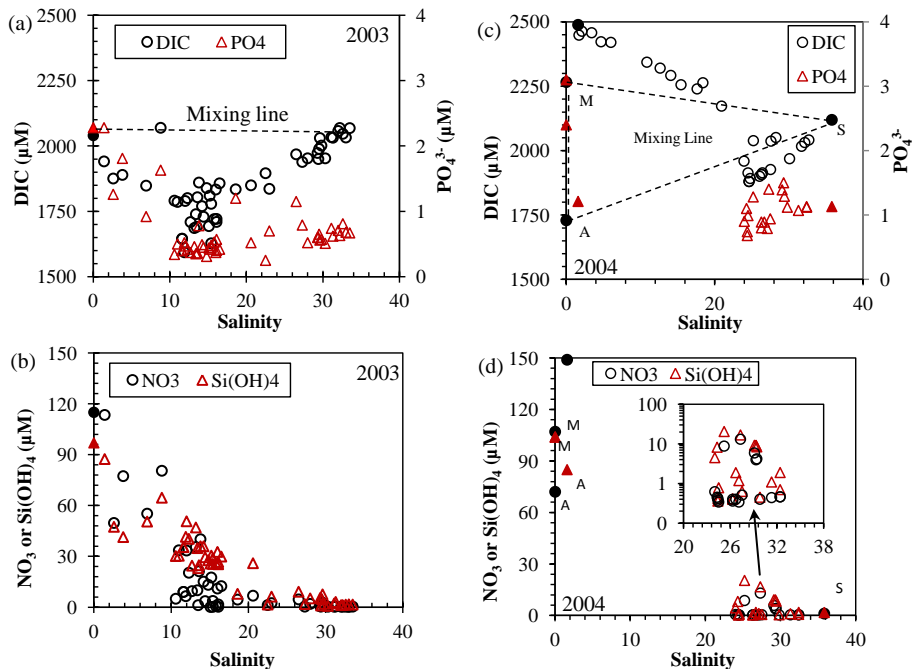
Title Page

Abstract | Introduction

Conclusions | References

Tables | Figures

|◄ | ►|

◄ | ►

Back | Close

Full Screen / Esc

Printer-friendly Version

Interactive Discussion

Fig. 3. Variation of DIC and nutrient concentrations along the salinity gradient. Panel **(a)** shows DIC and PO_4^{3-} versus salinity, respectively and panel **(b)** is NO_3 and $Si(OH)_4$ versus salinity, respectively, for June 2003. For August 2004, panel **(c)** shows DIC and PO_4^{3-} versus salinity, respectively and panel **(d)** is NO_3 and $Si(OH)_4$ versus salinity, respectively. Filled markers are the river endmembers. Dashed lines are the conservative mixing lines between the freshwater and sea endmembers for DIC versus salinity in panels **(a)** and **(c)**. Abbreviations "M", "A", and "S" in panels **(c)** and **(d)** have the same meanings as Fig. 2f. The insert figure in panel **(d)** enlarges the crowded area with logarithm scale in y-axis. Nutrient data for salinity less than 24 water were unavailable in August 2004.
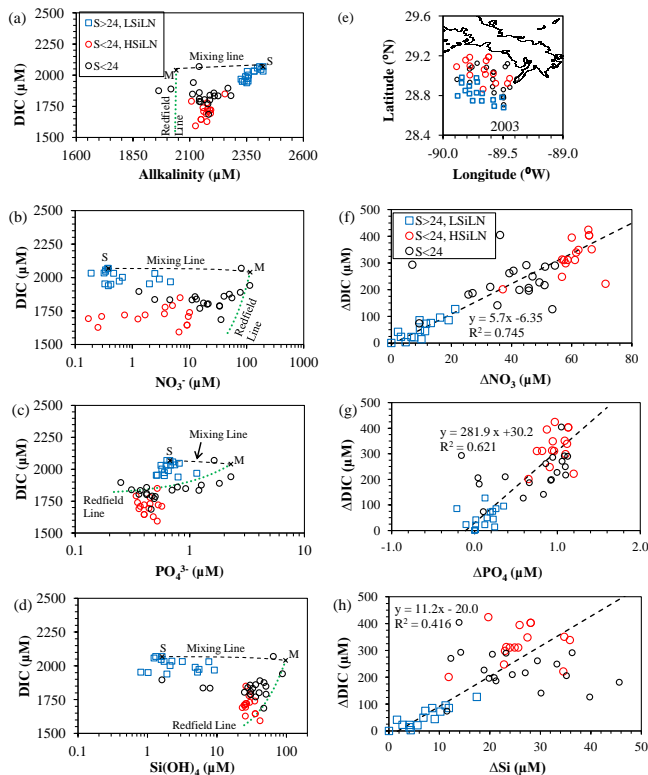
Fig. 4. Examine DIC, TA, nutrients, ΔDIC, and Δnutrients together with their sampling geographic locations for June 2003. Panels **(a)**–**(d)** show relationships of DIC to alkalinity, NO_3, PO_4^{3-}, and $Si(OH)_4$, respectively Black dash lines represent the conservative mixing lines and green dash lines are the Redfield-type biological removal line "X" markers with abbreviations "M", "A", and "S" are the same endmembers as in Fig. 3. Panel **(e)** shows the corresponding sampling sites for the other panels. Panels **(f)**–**(h)** show relationships of ΔDIC to ΔNO, ΔPO$_4$, and ΔSi, respectively. Dash lines are correlation lines. All panels share the same legends as in panel.
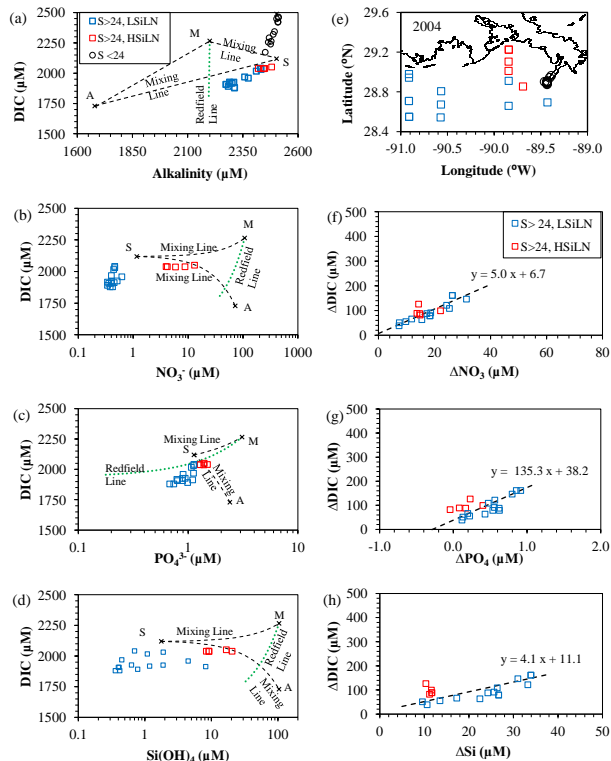
Fig. 5. Examine DIC, TA, nutrients, ΔDIC, and Δnutrients together with their sampling geographic locations for August 2004. Panels **(a)**–**(d)** show relationships of DIC to alkalinity, NO_3, PO_4^{3-}, and $Si(OH)_4$, respectively. Black dash lines represent the conservative mixing lines and green dash lines are the Redfield-type biological removal line "X" markers with abbreviations "M", "A", and "S" are the same endmembers as in Fig. 3. Panel **(e)** shows the corresponding sampling sites for the other panels. Panels **(f)**–**(h)** show relationships of ΔDIC to ΔNO, ΔPO$_4$, and ΔSi, respectively Dash lines are correlation lines. All panels share the same legends as in panel **(a)**.

Title Page

Abstract | Introduction

Conclusions | References

Tables | Figures

|◄ | ►|

◄ | ►

Back | Close

Full Screen / Esc

Printer-friendly Version

Interactive Discussion

Fig. 6. Si(OH)$_4$ to NO$_3$ and ΔSi to ΔNO$_3$ relationships. Panels **(a)** and **(b)** are Si(OH)$_4$ versus NO$_3$ plots for June 2003 and August 2004, respectively. Panel **(c)** is the ΔSi versus ΔNO$_3$ plot for June 2003 where the dashed lines are the linear regression relationships for both LSiLN, and HSiLN areas. Panel **(d)** is the ΔSi versus ΔNO$_3$ plot for August 2004 where the dashed line is the linear regression relationship for the LSiLN area and the solid line is the linear regression relationship for all data from August 2004. Panels of June 2003 **(a, b)** share the same legends as in Fig. 4. Panels of August 2004 **(d, e)** share the same legends as Fig. 5.